



RESEARCH ARTICLE

Bayesian model uncertainty quantification for hyperelastic soft tissue models

Milad Zeraatpisheh¹ , Stephane P.A. Bordas^{1,2*}  and Lars A.A. Beex¹ 

¹Institute of Computational Engineering, Faculty of Science, Technology and Communication, University of Luxembourg, Maison du Nombre, 6, Avenue de la Fonte, 4364 Esch-sur-Alzette, Luxembourg

²School of Engineering, Cardiff University, Queen's Buildings, The Parade, Cardiff CF243AA, United Kingdom

*Corresponding author. Email: stephane.bordas@uni.lu

Received: 09 March 2021; Revised: 17 May 2021; Accepted: 16 June 2021

Keywords: Model uncertainty; Bayesian inference; incompressible hyperelasticity; soft tissues

Abstract

Patient-specific surgical simulations require the patient-specific identification of the constitutive parameters. The sparsity of the experimental data and the substantial noise in the data (e.g., recovered during surgery) cause considerable uncertainty in the identification. In this exploratory work, parameter uncertainty for incompressible hyperelasticity, often used for soft tissues, is addressed by a probabilistic identification approach based on Bayesian inference. Our study particularly focuses on the uncertainty of the model: we investigate how the identified uncertainties of the constitutive parameters behave when different forms of model uncertainty are considered. The model uncertainty formulations range from uninformative ones to more accurate ones that incorporate more detailed extensions of incompressible hyperelasticity. The study shows that incorporating model uncertainty may improve the results, but this is not guaranteed.

Impact Statement

Bayesian inference is increasingly discussed to identify the constitutive models' parameters of soft tissue. However, sometimes the obtained parameters cannot predict the behavior of soft tissues. Therefore, in this work, the effect of incorporating "Model uncertainty" to reduce the mismatch between reality and model prediction has been explored.

1. Introduction

Constitutive models of soft tissues are crucial for computer-aided surgery, surgical training simulators, functional tissue engineering, and traumatic brain injury simulations (Humphrey, 2003; Madireddy et al., 2015; Hauseux et al., 2018; Bui et al., 2019; Duprez et al., 2020; Magliulo et al., 2020). Although several sophisticated constitutive models for soft tissues were proposed (Courtney et al., 2006; Guo et al., 2006), soft tissues are still often described using incompressible hyperelasticity. The simplicity of incompressible hyperelasticity has the advantage that few parameters need to be identified. The soft tissue models in this contribution are limited to incompressible hyperelasticity.

Parameter values of a soft tissue model identified during surgery may not be accurate, because the experimental data are sparse and affected by a substantial amount of measurement noise (due to the limitations of the type of observations and the sampling frequency of the observations). The uncertainties of the parameter values are, therefore, important to consider. Although conventional probabilistic identification frameworks can identify parameter uncertainties, they are traditionally not formulated to account for the fact that the model itself is limited to describe the data. To overcome this deficiency, model uncertainty can be incorporated in probabilistic identification frameworks.

Model uncertainty can be defined as the uncertainty due to the inability of a model to describe observations of the real world. Model uncertainty comes into play if a discrepancy between the model and the experimental data is present that cannot be explained by the noise in the data. A well-accepted approach to include the uncertainty of models in probabilistic identification settings was presented by Kennedy and O'Hagan (KOH) (Kennedy and O'Hagan, 2001). This "KOH" framework was, for instance, employed in (Arhonditsis et al., 2008; Higdon et al., 2008; McFarland and Mahadevan, 2008; Sankararaman et al., 2011; Arendt et al., 2012).

In the present work, we develop a KOH framework (able to treat both the uncertainty of the data and the uncertainty of the model) to identify uncertainties of the parameters of incompressible hyperelasticity. The aim is to investigate how different formulations of model uncertainty influence the identified parameter uncertainties. For this purpose, different model uncertainty formulations have been considered. These formulations range from uninformative to probabilistically more advanced ones, and from input-independent forms to formulations based on more advanced *incompressible hyperelasticity*. In this contribution, we consider synthetic data, so that we can make a quantitative comparison with the reference input. As this study is exploratory, we limit ourselves to tensile and compression data for which the model responses can be described by closed-form expressions.

1.1. Bayesian updating and its application in solid mechanics

Parameter identification is still largely performed in deterministic settings such as the method of least squares (Loh and Das, 1986; Wu and Lee, 2006; Ortiz et al., 2011; Beex, 2019; Loew et al., 2020). The result of a deterministic identification procedure, such as least squares, is a single set of parameter values. This set is the most probable set of parameter values, assuming, for instance, that no discrepancy between model and measurements exists and that the noise is symmetrically distributed.

Probabilistic identification approaches aim to identify not only the most probable set of parameter values, but all sets of parameter values that may have produced the measured data. In other words, they aim to determine the probability of each set of parameter values. This is accomplished by identifying a probability density function (PDF) in terms of the model parameters. Instead of identifying material parameters, a PDF must be evaluated.

One probabilistic identification approach is Bayesian inference (BI), which is based on Bayes' theorem. In BI, an initial PDF in terms of the constitutive parameters must be defined by the user. This initial PDF incorporates all a priori knowledge. This a priori knowledge can be relatively uninformative, for example, by stating that Young's modulus cannot be negative, but it can also be more informative. For instance, if one knows that a cortical bone is considered, Young's modulus is probably between 15 and 25 GPa.

In BI, the initial PDF (i.e., the prior) is updated by inferring the experimental data. This commonly entails that the noise distribution must be identified beforehand (Rappel et al., 2020). However, the parameters of the noise distribution may also be treated as parameters that are to be simultaneously identified with the model parameters.

The final PDF that results from BI is called the posterior and is often so complex that the associated cumulative distribution function cannot be analytically expressed—entailing that sets of constitutive parameters cannot be randomly generated from the posterior. In those cases, the posterior is typically explored by seeding numerous samples and evaluating the PDF for each sample. Several numerical frameworks have been proposed in the past to limit the number of

necessary samples (in order to decrease the computational cost of the numerical sampling). Well-known examples are Markov chain Monte Carlo techniques (Higdon et al., 2002; Wang and Zabaras, 2004; Risholm et al., 2013; Lan et al., 2016) and hybrid Monte Carlo (HMC) methods (Beskos et al., 2013; Betancourt, 2017).

One of the earlier works in which BI is exploited to identify parameter uncertainties in computational mechanics is that of Isenberg (Isenberg, 1979), in which it was used to identify elastic parameters in 1979. In other works, the framework was employed to identify elastic material parameters based on dynamic responses (Alvin, 1997; Beck and Katafygiotis, 1998; Marwala and Sibisi, 2005; Mohamedou et al., 2019). BI was also used to identify the elastic constants of composites (Lai and Ip, 1996; Daghia et al., 2007; Nichols et al., 2010; Gogu et al., 2013). Spatially varying elastic parameters were, furthermore, identified using BI by Koutsourelakis (2012) and Hussein et al. (2019). The Bayesian paradigm was also used for the identification of parameter uncertainties of constitutive models (Rappel et al., 2018; Rappel et al., 2019; Rappel and Beex, 2019; Teferra and Brewick, 2019).

Two works have previously applied BI for the parameter identification of hyperelastic models (Madireddy et al., 2015; Madireddy et al., 2016). Madireddy et al. (2015) considered three hyperelastic models for soft tissues and investigated the effect of the uncertainty on a quantity of interest. On the other hand, Ritto and Nunes (2015) exploited BI not only to identify parameter distributions, but also to select which hyperelastic model is most suited.

The difference between our contribution and the works of Madireddy et al. (2015) and Ritto and Nunes is that we aim to investigate how the incorporation of different forms of model uncertainty affects the identified material parameter distributions. The reason that model uncertainty is relevant is that although probabilistic identification approaches identify the probability of all (meaningful) sets of material parameters (instead of only the most probable set), they are commonly based on the same assumption as deterministic identification approaches: *the model is able to describe the observed data*. Hence, even probabilistic identification approaches must be extended in order to treat the possible uncertainty of the model.

The structure of the study is as follows: in Section 2, we summarize the employed material models. In Section 3, we discuss BI in more detail, as well as the different types of model uncertainty that are investigated. Afterward, the results are presented, and finally, the study is closed with a conclusion.

2. Material Models

In the present work, BI is used to identify the parameters of arguably the simplest incompressible hyperelastic model: the Neo-Hookean model. As the part of the Mooney–Rivlin model and the Yeoh model that are not present in Neo-Hookean hyperelasticity are later considered as forms of model uncertainty, we also discuss them.

2.1. A family of incompressible hyperelasticity models

The mapping of the location of a material point from the reference configuration, \mathbf{X} , to the location in the deformed configuration, \mathbf{x} , is described by $\mathbf{x} = \chi(\mathbf{X})$. The deformation gradient tensor is defined as $\mathbf{F} = \frac{\partial \mathbf{x}}{\partial \mathbf{X}}$. The eigenvalues of the deformation gradient tensor are defined as principal stretches $\lambda_k, k = 1, 2, 3$. The right Cauchy–Green deformation tensor (Green’s deformation tensor) and its three invariants can then be computed as follows:

$$\mathbf{C} = \mathbf{F}^T \mathbf{F}, \quad (1)$$

$$I_1(\mathbf{C}) = \text{trace}(\mathbf{C}), \quad (2)$$

$$I_2(\mathbf{C}) = \frac{1}{2} \left(I_1(\mathbf{C})^2 - \text{trace}(\mathbf{C}^2) \right), \quad (3)$$

$$I_3 = \det(\mathbf{C}). \quad (4)$$

One family of incompressible hyperelastic models is given by the following set of strain energy density functions:

$$\sum_{i,j=0}^n C_{ij}(I_1 - 3)^i(I_2 - 3)^j, \quad (5)$$

where C_{ij} denote material parameters and $C_{00} = 0 \text{ Pa}$. The Neo-Hookean material model is obtained by setting $n = 1$, $C_{01} = 0$, and $C_{11} = 0$, so that only one parameter, C_{10} , remains. The standard Mooney–Rivlin material model is also obtained by setting $n = 1$, but $C_{01} \neq 0$, so that two material parameters govern its behavior: C_{10} and C_{01} . The Yeoh model is obtained by setting $n = 3$ and $C_{01} = C_{02} = C_{03} = C_{11} = C_{12} = C_{13} = C_{21} = C_{22} = C_{23} = C_{31} = C_{32} = C_{33} = 0 \text{ Pa}$, so that three parameters remain: C_{10} , C_{20} , and C_{30} .

2.2. Expressions for the measured stress during tensile tests

By differentiating the Neo-Hookean strain energy density with respect to the deformation gradient tensor and converting the resulting stress tensor (the first Piola–Kirchhoff stress tensor) to the Cauchy stress tensor, the nonzero component of the Cauchy stress in uniaxial tension/compression can be expressed as follows:

$$\sigma_{\text{Cauchy}} = 2C_{10}(\lambda^2 - \lambda^{-1}), \quad (6)$$

where λ denotes principal stretch in the direction in which the tension/compression is applied. The engineering stress that is observed in a uniaxial experiment then reads:

$$\sigma = 2C_{10}(\lambda - \lambda^{-2}). \quad (7)$$

For the standard Mooney–Rivlin model, applying the same procedure as for the Neo-Hookean model results in the following expression for the nonzero component of the Cauchy stress during a tension/compression experiment:

$$\sigma_{\text{Cauchy}} = 2C_{10}(\lambda^2 - \lambda^{-1}) + 2C_{01}(\lambda - \lambda^{-2}), \quad (8)$$

which results in the following engineering stress that is actually observed:

$$\sigma = 2C_{10}(\lambda - \lambda^{-2}) + 2C_{01}(1 - \lambda^{-3}). \quad (9)$$

Using the same procedure for the Yeoh model, we arrive at the following expression for the nonzero Cauchy stress in case of uniaxial extension/compression:

$$\begin{aligned} \sigma_{\text{Cauchy}} = & 2C_{10}(\lambda^2 - \lambda^{-1}) + 4C_{20}(\lambda^4 - 3\lambda^2 + \lambda + 3\lambda^{-1} - 2\lambda^{-2}) + \\ & 6C_{30}(\lambda^6 - 6\lambda^4 + 3\lambda^3 + 9\lambda^2 - 6\lambda - 9\lambda^{-1} + 12\lambda^{-2} - 4\lambda^{-3}), \end{aligned} \quad (10)$$

resulting in the following engineering stress observable during a uniaxial tensile test:

$$\begin{aligned} \sigma = & 2C_{10}(\lambda - \lambda^{-2}) + 4C_{20}(\lambda^3 - 3\lambda + 1 + 3\lambda^{-2} - 2\lambda^{-3}) + \\ & 6C_{30}(\lambda^5 - 6\lambda^3 + 3\lambda^2 + 9\lambda - 6 - 9\lambda^{-2} + 12\lambda^{-3} - 4\lambda^{-4}). \end{aligned} \quad (11)$$

It should be noted that in real application of using Bayesian paradigm, forward simulation are computationally expensive; therefore, data-driven model can be used to replace complex forward simulations (Bigoni et al., 2020; Mendizabal et al., 2020; however, the forward simulations are out of scope of the current contribution, as it is a subdomain in its own right).

3. Bayesian Parameter Identification

Bayes' theorem provides a consistent way to quantify the probability of an event by incorporating both one's prior knowledge (described by a PDF, the prior) and observed measurements (also described by a

PDF, the likelihood function). Suppose $\underline{d}^T = [d_1, \dots, d_{n_m}]$ denotes the n_m measurements, and $\underline{\theta}^T = [\theta_1, \dots, \theta_{n_p}]$ the n_p parameters (which are to be identified). Bayes' theorem can then be written as follows:

$$P(\underline{\theta}|\underline{d}) = \frac{P(\underline{\theta})P(\underline{d}|\underline{\theta})}{P(\underline{d})}, \quad (12)$$

where $P(\underline{\theta})$ denotes the prior distribution, the PDF that quantifies one's assumed knowledge about the parameters. As the prior distribution can be constructed before the measurements are made, it is independent of the measurements. $P(\underline{d}|\underline{\theta})$ denotes the likelihood function and describes the probability of measurements \underline{d} , given parameters $\underline{\theta}$. $P(\underline{\theta}|\underline{d})$ denotes the posterior distribution that describes the plausibility of parameters $\underline{\theta}$, given measurements \underline{d} . The posterior is our PDF of interest: it quantifies the probability of each set of parameter values. $P(\underline{d})$ is called the evidence, and since it is independent of the model parameters (i.e., random variables), $\underline{\theta}$, it can be replaced by a positive scalar ($a \in \mathbb{R}^+$):

$$P(\underline{\theta}|\underline{d}) = \frac{P(\underline{\theta})P(\underline{d}|\underline{\theta})}{a}. \quad (13)$$

Considering that the statistical summaries of the posterior distribution (e.g., the mean, the covariance matrix, and the maximum-a-posteriori estimate) are only affected by the shape of the posterior distribution and not by its magnitude, if the posterior is numerically sampled (which is the case here). Therefore, the following expression can be used instead of Equation (13) (Rappel et al., 2020):

$$P(\underline{\theta}|\underline{d}) \propto P(\underline{\theta})P(\underline{d}|\underline{\theta}). \quad (14)$$

To construct the likelihood function, we directly incorporate the fact that the discrepancy between the measured stress (σ^m) and the stress predicted by the model (σ) is not only caused by a statistical error governed by the experimental equipment (Ω_{noise}), but also by an inability of the model to describe the measurements. The term describing this inability, that is, the model uncertainty, is denoted by M and depends on its own parameters, $\underline{\theta}_M$. Assuming an additive decomposition of the model and the model uncertainty, we write the following expression for a stress measurement:

$$\sigma^m = \sigma(\lambda, \underline{\theta}) + M(\underline{\theta}_M) + \Omega_{\text{noise}}, \quad (15)$$

wherever λ denotes the input (the principal stretch in the direction in which tension is applied) for which the output (σ^m) was measured. σ denotes the stress-principle stretch relation for Neo-Hookean hyper-elasticity during uniaxial tension/compression (Equation (7)). Hence, the likelihood function for a single measurement now reads:

$$P(d_i|\underline{\theta}, \underline{\theta}_M) = P_{\text{noise}}(d_i - \sigma(\lambda_i|\underline{\theta}) - M(\underline{\theta}_M)). \quad (16)$$

As we know that:

$$P_{\text{noise}}(\Omega_{\text{noise}}) = \frac{1}{\Sigma_{\text{noise}}} \exp\left(\frac{-\Omega_{\text{noise}}^2}{2\Sigma_{\text{noise}}^2}\right), \quad (17)$$

where we ignored $\sqrt{2\pi}$ for the normalization, because the scaling in Equation (17) makes this constant value irrelevant. We will also ignore this for all following likelihood functions.

In the present work, like in many other studies, the noise distribution is considered to be Gaussian with a zero mean and a known variance, Σ_{noise}^2 . Often the parameters of the model uncertainty, $\underline{\theta}_M$, are unknown and should be identified alongside the model parameters.

Considering Equations (15) and (16), the posterior distribution for one measurement reads:

$$P(\underline{\theta}, \underline{\theta}_M | d_i) \propto P(\underline{\theta})P(\underline{\theta}_M)P_{\text{noise}}(d_i - \sigma(\lambda_i|\underline{\theta}) - M(\underline{\theta}_M)), \quad (18)$$

where $P(\underline{\theta}_M)$ and $P(\underline{\theta})$ denote the prior for the model uncertainty parameters and the prior for the model parameters, respectively. It should be noted that in Equation (18), the model uncertainty parameters and the model parameters are assumed to be independent.

The final likelihood function for n_m independent measurements is obtained by multiplying the likelihood functions of each measurement:

$$P(\underline{d}|\underline{\theta}, \underline{\theta}_M) = \prod_{i=1}^{n_m} P_{\text{noise}}(d_i - \sigma(\lambda_i, \underline{\theta}) - M(\underline{\theta}_M)). \quad (19)$$

4. Model Uncertainty

In the previous section, we constructed the general expression of a likelihood function (and posterior) including an unspecified model uncertainty. In this section, we present the general expressions of the posteriors for different types of model uncertainty.

Six model uncertainty formulations are considered:

1. A random variable associated with a normal distribution with a constant mean and variance;
2. A random variable associated with a normal distribution with a linear input-dependent (stretch-dependent) mean;
3. A random variable associated with a normal distribution with a quadratic input-dependent mean;
4. A random variable associated with the second term of Mooney–Rivlin hyperelasticity;
5. A random variable associated with the last two terms of Yeoh hyperelasticity;
6. A Gaussian process (GP) with a stationary covariance function.

4.1. Normal distribution with constant mean

In the first scenario, the model uncertainty is expressed as a normal distribution with mean m and variance Σ^2 (i.e., $\underline{\theta}_M = [m, \Sigma]^T$). Hence, these two parameters should be identified alongside the model parameters. The likelihood distribution for a single measurement, $d_i = \sigma_i^m$ (Equation (18)), can now be written as follows:

$$P(d_i|\underline{\theta}, \underline{\theta}_M) = \frac{1}{\sqrt{\Sigma_{\text{noise}}^2 + \Sigma^2}} \exp\left(\frac{-(d_i - \sigma(\lambda_i, \underline{\theta}) - m)^2}{2(\Sigma_{\text{noise}}^2 + \Sigma^2)}\right). \quad (20)$$

4.2. Normal distribution with a linear mean

The second case of model uncertainty is the same as the first case, except that the mean is linearly dependent on the input. To this end, the likelihood function for a single measurement, $d_i = \sigma_i^m$, is written as follows:

$$P(d_i|\underline{\theta}, \underline{\theta}_M) = \frac{1}{\sqrt{\Sigma_{\text{noise}}^2 + \Sigma^2}} \exp\left(\frac{-(d_i - \sigma(\lambda_i, \underline{\theta}) - m_0 + m_1\lambda_i)^2}{2(\Sigma_{\text{noise}}^2 + \Sigma^2)}\right). \quad (21)$$

Clearly, $\underline{\theta}_M = [m_0, m_1, \Sigma]^T$.

4.3. Normal distribution with a quadratic mean

In the next case, the same model uncertainty is again considered, yet the expression of the mean is again changed: a quadratic expression is used, resulting in the following likelihood function for a single measurement:

$$P(d_i|\underline{\theta}, \underline{\theta}_M) = \frac{1}{\sqrt{\Sigma_{\text{noise}}^2 + \Sigma^2}} \exp\left(\frac{-(d_i - \sigma(\lambda_i, \underline{\theta}) - m_0 - m_1\lambda_i - m_2\lambda_i^2)^2}{2(\Sigma_{\text{noise}}^2 + \Sigma^2)}\right). \quad (22)$$

Therefore, $\underline{\theta}_M = [m_0, m_1, m_2, \Sigma]^T$.

4.4. Mooney–Rivlin hyperelasticity

In the fourth case, model uncertainty is chosen in the same way as before, except that the mean behaves according to the second term of standard Mooney–Rivlin hyperelasticity. As the stress–stretch relation for standard Mooney–Rivlin hyperelasticity in a tensile/compression experiment is expressed according to [Equation \(9\)](#), the likelihood function for a single measurement is now expressed as follows:

$$P(d_i|\underline{\theta}, \underline{\theta}_M) = \frac{1}{\sqrt{\Sigma_{\text{noise}}^2 + \Sigma^2}} \exp \left(\frac{-(d_i - \sigma(\lambda_i, \underline{\theta}) - 2C_{01}(1 - \lambda_i^{-3}))^2}{2(\Sigma_{\text{noise}}^2 + \Sigma^2)} \right), \quad (23)$$

where we repeat for clarity that the expression for $\sigma(\lambda_i, \underline{\theta})$ is given in [Equation \(7\)](#). In this case, $\underline{\theta}_M = [C_{01}, \Sigma]^T$.

4.5. Yeoh model

The fifth case is the same as the previous cases, except that the mean is now taken as the last two terms of Yeoh hyperelasticity. This type of model uncertainty is of course chosen here, because we know that the synthetic data are generated using Yeoh hyperelasticity, but also in a real-world scenario, it makes sense to use a more advanced model than Neo-Hookean hyperelasticity (or Mooney–Rivlin hyperelasticity) for that matter as it gives almost the same response for uniaxial tension as Neo-Hookean hyperelasticity). This yields the following likelihood function for a single measurement:

$$P(d_i|\underline{\theta}, \underline{\theta}_M) = \frac{1}{\sqrt{\Sigma_{\text{noise}}^2 + \Sigma^2}} \exp \left(\frac{-(d_i - \sigma(\lambda_i, \underline{\theta}) - 2[2C_{20}(\lambda_i^3 - 3\lambda_i + 1 + 3\lambda_i^{-2} - 2\lambda_i^{-3} + \dots) \right. \\ \left. - \dots + 3C_{30} + (\lambda_i^5 - 6\lambda_i^3 + 3\lambda_i^2 + 9\lambda_i - 6 - 9\lambda_i^{-2} + 12\lambda_i^{-3} - 4\lambda_i^{-4}])^2}{2(\Sigma_{\text{noise}}^2 + \Sigma^2)} \right) \\ \exp \left(\frac{(\dots + 3C_{30} + (\lambda_i^5 - 6\lambda_i^3 + 3\lambda_i^2 + 9\lambda_i - 6 - 9\lambda_i^{-2} + 12\lambda_i^{-3} - 4\lambda_i^{-4}))^2}{2(\Sigma_{\text{noise}}^2 + \Sigma^2)} \right). \quad (24)$$

In this case, $\underline{\theta}_M = [C_{20}, C_{30}, \Sigma]$.

4.6. Gaussian process

In the last case, we consider model uncertainty in the form of a GP with a zero mean. GP provides a solution to modeling arbitrary function by letting the data choose the complexity of the response. This form of model uncertainty is inherently different from the previous ones, because it involves a correlation between all the inputs. Consequently, the final likelihood function cannot be formulated as a multiplication of different likelihood functions, each associated with a single measurement (i.e., [Equation \(20\)](#) cannot be used). Instead, the final likelihood function must directly be expressed for all n_m measurements. The final likelihood function reads:

$$P(d|\underline{\theta}, \underline{\theta}_M) = \frac{1}{|\underline{\Sigma} + \Sigma_{\text{noise}} \underline{I}|} \exp \left(-\frac{1}{2} (\underline{d} - \underline{\sigma}(\lambda, \underline{\theta}))^T (\underline{\Sigma} + \Sigma_{\text{noise}} \underline{I})^{-1} (\underline{d} - \underline{\sigma}(\lambda, \underline{\theta})) \right), \quad (25)$$

where $|\cdot|$ denotes the determinant of a matrix, \underline{I} an $n_m \times n_m$ diagonal identity matrix, and $\underline{\Sigma}$ the $n_m \times n_m$ (symmetric) covariance matrix associated with the GP, of which the component at row i , column j is formulated as follows:

$$(\underline{\Sigma})_{ij} = c^2 \exp \left(\frac{-(\lambda_i - \lambda_j)^2}{2\psi^2} \right). \quad (26)$$

Two model uncertainty parameters are, therefore, associated with the GP: $\underline{\theta}_M = [c, \psi]^T$.

5. Results

In this section, the results for the different forms of model uncertainty are compared to each other. The measurement data are artificially generated (it is supposed that experimental data are not correlated) with the Yeoh model with $C_{10} = 1.2\text{MPA}$, $C_{20} = -0.057\text{MPA}$, and $C_{30} = 0.004\text{MPA}$. The measurement noise is generated using a normal distribution with a zero-mean variance of $\Sigma_{\text{noise}} = 0.5\text{MPA}$. The model of interest is Neo-Hookean hyperelasticity, entailing that we are interested in parameter C_{10} .

In the diagrams that follow below, both the posterior predictive (PP) check and the highest-posterior density (HPD; also known as the credible interval) are presented. The PP check generates “new observations,” although they are presented as bands in the diagrams below. The new observations can be used to interpolate or extrapolate the model or to investigate whether or not the model is able to emulate the (old) measurements that were used to identify its parameters and uncertainties. The former is performed (i.e., assessing if the old measurements are within the same band as the new measurements).

In order to generate the new observations, the PP check uses the posterior distribution and the noise distribution (i.e., the likelihood function) as follows:

$$P(\hat{d}|d) = \int \int P(\hat{d}|\underline{\theta}, \underline{\theta}_M) P(\underline{\theta}, \underline{\theta}_M|d) d\underline{\theta} d\underline{\theta}_M, \quad (27)$$

where \hat{d} denotes a new measurement.

To work out the integral in Equation (27), one can first take a sample for $\underline{\theta}$ and $\underline{\theta}_M$ from posterior distribution $P(\underline{\theta}|d)$, and then use this sample in the likelihood function to obtain the new measurement, \hat{d} .

The HPD interval is a commonly used method to explain the spread of the posterior distribution. The smallest interval containing an X percent of the probability density is called the $X\%$ HPD. In the present contribution, the 95% HPD is used to compare the influence of the different forms of model uncertainty.

It should be noted that in all parts of this study, an uninformative prior distribution (i.e., a uniform distribution) with a wide interval is used, which implies that the posterior is effectively governed by the inference of the experimental data.

It is also worth to note that in order to obtain the results of this section, all posteriors are numerically sampled. Instead of a random walk sampler, such as the Metropolis–Hastings algorithm, an HMC sampler is used. Where random walk samplers only require posterior evaluations, HMC samplers also require the gradient of the posterior. Thanks to the gradient information, HMC samplers need less samples to evaluate posteriors than random walk samplers, entailing that HMC samplers are an order of magnitude faster than random walk samplers (Beskos et al., 2013; Betancourt, 2017).

5.1. Polynomial model uncertainty

Figure 1a presents the PP check for Neo-Hookean hyperelasticity without any model uncertainty. It is clear that the previous measurements are not contained in the bands formed by the new measurements. This stems from the fact that the synthetic data are generated from Yeoh hyperelasticity. Figure 1b, c makes clear that incorporating model uncertainty as a normal distribution with a constant mean or a linear input-dependent mean hardly changes the results. For the linear input-dependent mean, this can be explained by the fact that the Neo-Hookean response itself also contains a linear dependency. If model uncertainty consists of a normal distribution with a quadratic input-dependent mean, the results are substantially better (Figure 1d). This can be explained by the fact that the quadratic dependency of the model uncertainty is not present in the Neo-Hookean response.

We believe that it is interesting to reveal how much of the “work” to generate the new measurements (according to the PP check) is performed by the model and how much by the model uncertainty. To this end, Figure 2 presents the PP check by considering that only the model is used to generate the new observations. In other words, even though the probabilistic identification is performed using model uncertainty, Equation (27) is replaced by:

$$P(\hat{d}, d) = \int P(\hat{d}|\underline{\theta}) P(\underline{\theta}|d) d\underline{\theta}. \quad (28)$$

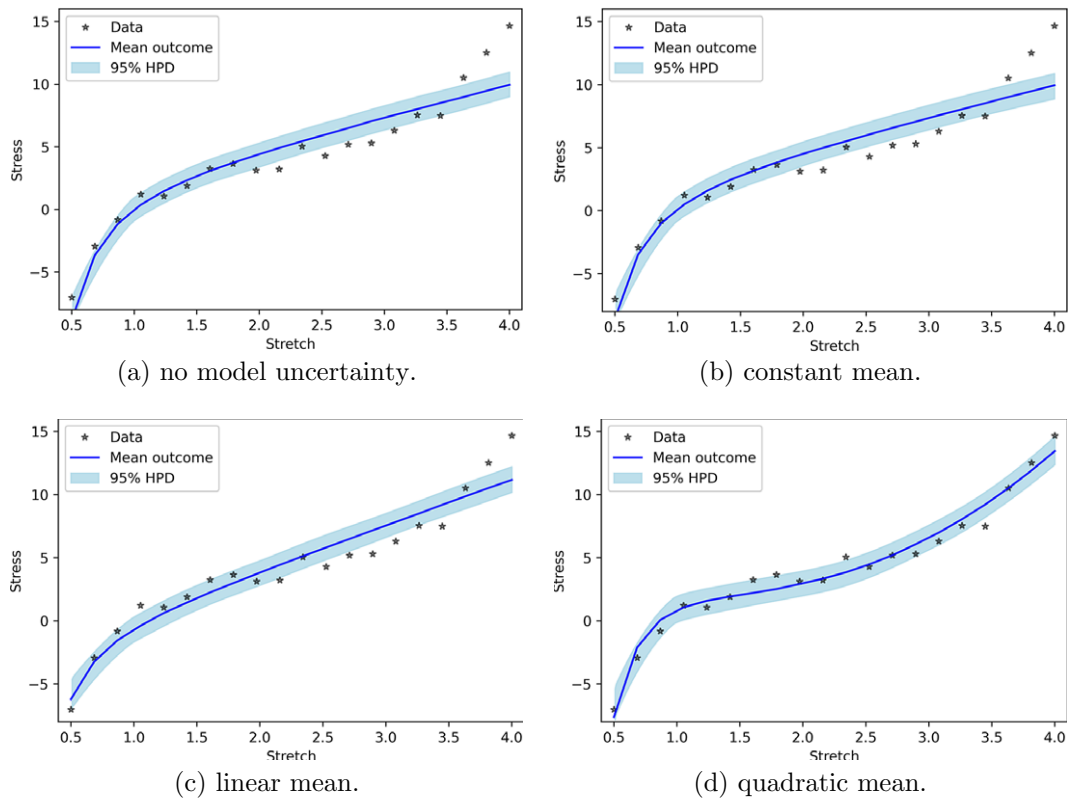


Figure 1. posterior predictive check for polynomial model uncertainty.

It is easy to see that in case of a constant and a linear input-dependent mean, the model uncertainty hardly performs any work. In case of the quadratic input-dependent mean, on the other hand, the model uncertainty can substantially improve the prediction.

5.2. Hyperelastic model uncertainty

In this part, we consider model uncertainty as a normal distribution with an input-dependent mean where the input-dependency follows the response of more complex hyperelastic models than Neo-Hookean hyperelasticity. We consider the mean to behave according to the parts of the Mooney–Rivlin response and the Yeoh response that are not present in the Neo-Hookean response. Figure 3b shows that the PP checks of Mooney–Rivlin model uncertainty and without model uncertainty are practically the same. This can be explained by the fact that the uniaxial tensile/compression responses of Neo-Hookean and Mooney–Rivlin hyperelasticity are similar. Consequently, a mean according to the part of the Mooney–Rivlin response that is not present in the Neo-Hookean response hardly improves the prediction. As the part of the Yeoh response for uniaxial loading that is not present in the Neo-Hookean response is substantially different from the Neo-Hookean response, Yeoh model uncertainty relatively accurately describes the mismatch between model and measured data (Figure 3c).

In order to again reveal to which amount the new measurements of the PP check are due to the work of the model and the model uncertainty, we present the PP check for the model alone (i.e., according to Equation (28)). Figure 4 presents these results. Figure 4 shows that the improvement in Figure 3c is due to the effect of model uncertainty terms and not the model itself.

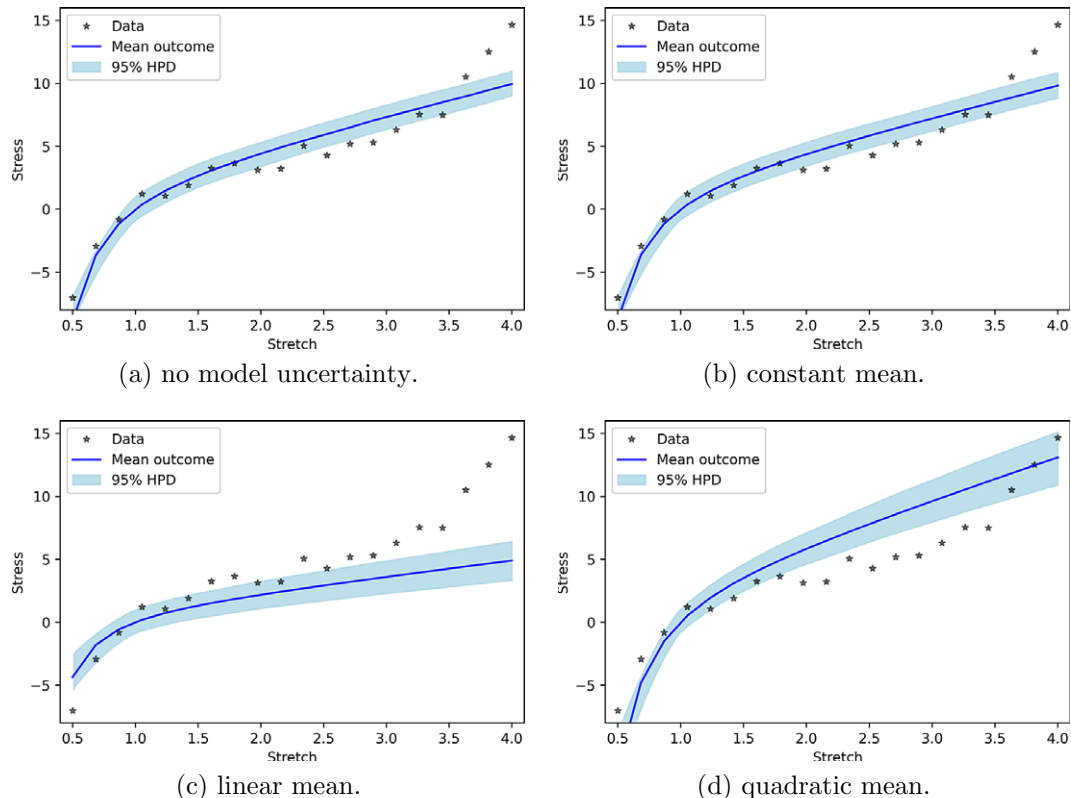


Figure 2. Posterior prediction for polynomial model uncertainty functions without work done by model uncertainty.

5.3. Gaussian process as model uncertainty

As the last case, model uncertainty is considered as a GP. In this model, no a priori shape (linear, quadratic, or etc.) imposed on the model uncertainty, and we let the GP to decide its shape. Figure 5 shows the PP for the GP model uncertainty. One can see that the results are completely in line with the measured data. In addition, similar to previous cases, Figure 6 indicates that the performance of Neo-Hookean hyperelasticity itself without considering the GP parameters are poor.

5.4. Marginal posteriors

Model uncertainty is often used to achieve a better fit between the PP check and the old measurements, assuming one is solely interested in the responses of Figures 1, 3, and 5. In computational (bio)mechanics, the aim is to use model uncertainty to make predictions for other models than the ones used to identify the parameter uncertainties (e.g., to use the identified parameter uncertainty for finite element simulations). In other words, we aim to employ model uncertainty not to make the PP check better fit the old measurements, but to ensure that the uncertainty of C_{10} is better identified.

From this perspective, the aforementioned PP checks (Figures 1, 3, and 5) are not the main interest (which is why we have also shown PP checks without the influence of model uncertainty in Figures 2, 4, and 6), but the marginal posteriors with respect to C_{10} . Figure 7 depicts the marginal posteriors with respect to C_{10} for different types of model uncertainty. It is clearly visible that the marginal posterior for the Yeoh model as model uncertainty incorporates the true value close to true value. Constant mean model uncertainty estimates C_{10} similar to the based model prediction. Another interesting point is that although quadratic mean was successfully passed the PP check, it cannot predict C_{10} .

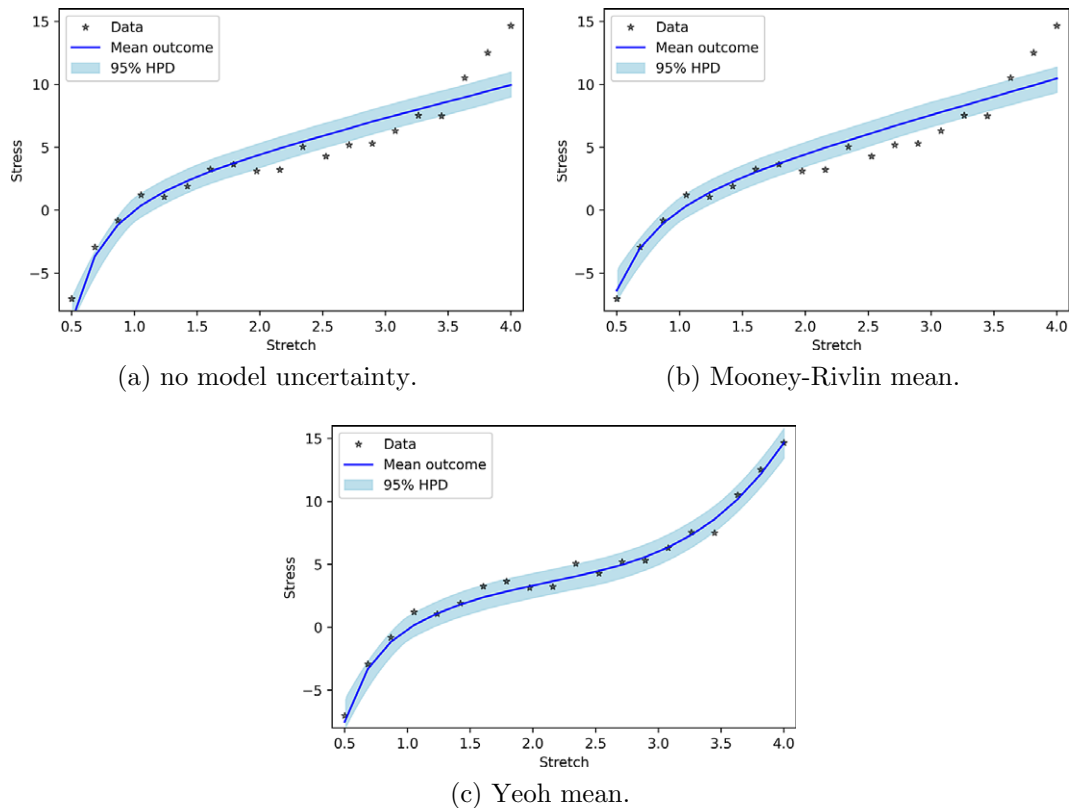


Figure 3. Posterior prediction for hyperelastic model uncertainty functions.

6. Conclusion

In this work, a Bayesian paradigm is employed to identify the parameter uncertainties of Neo-Hookean incompressible hyperelasticity based on tensile/compression data. (Synthetic data were generated in order to enable a quantitative comparison.) The aim of the work was to investigate the influence of different forms of model uncertainties. To this end, we have studied six types of model uncertainties:

1. A random variable associated with a normal distribution with a constant mean and variance;
2. A random variable associated with a normal distribution with a linear input-dependent (stretch-dependent) mean;
3. A random variable associated with a normal distribution with a quadratic input-dependent mean;
4. A random variable associated with the second term of Mooney–Rivlin hyperelasticity;
5. A random variable associated with the last two terms of Yeoh hyperelasticity;
6. A GP with a stationary covariance function.

Two lessons can be learned from this study. First, the fact that old measurements fall well within the bandwidth of the posterior predictions does not mean that the parameter uncertainties encompass the true parameter value(s). This was the case for model uncertainty modeled as a GP and for model uncertainty modeled as a random variable coming from a normal distribution with a quadratic input-dependent mean.

Second, incorporating model uncertainty does not guarantee that the parameter uncertainties encompass the true parameter value(s) better. We have observed that of the six types of model uncertainties, only two (model uncertainty as Yeoh hyperelasticity and model uncertainty as a random variable coming from

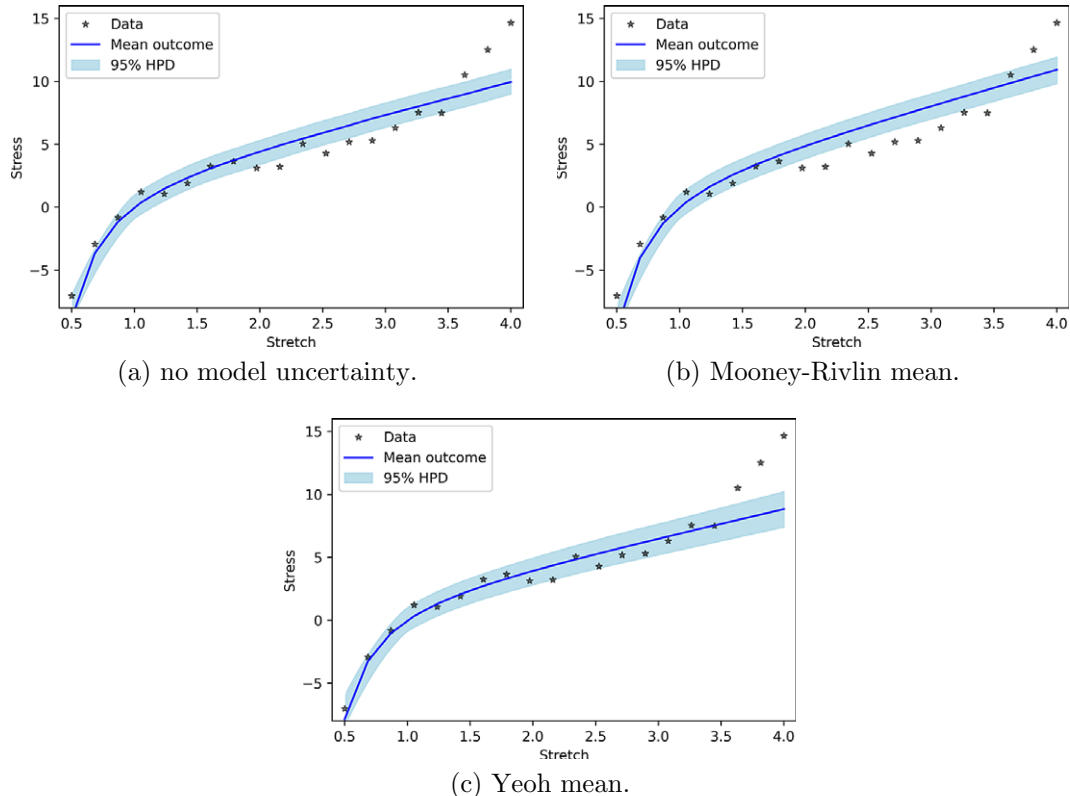


Figure 4. Posterior prediction for hyperelastic model uncertainty functions without work done by model uncertainty.

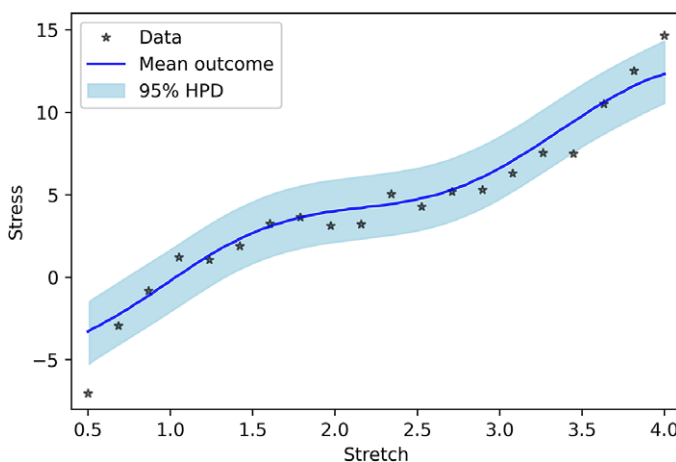


Figure 5. Posterior prediction for considering Gaussian process as model uncertainty.

a normal distribution with a constant mean) encompass the true value better than ignoring model uncertainty altogether.

The fact that, in most of the cases, model uncertainty yielded worse results shows, on the one hand, that it should only be used in a careful manner. For incompressible hyperelasticity, it seems that a more

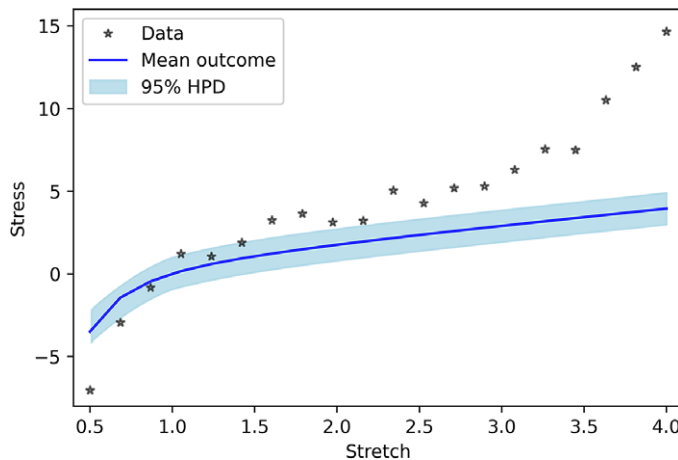


Figure 6. Posterior prediction for Gaussian process without work done by model uncertainty.

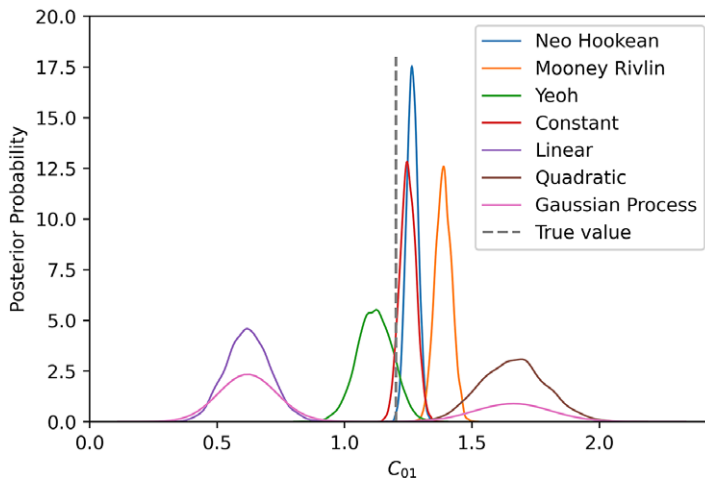


Figure 7. Marginal posteriors for C_{10} .

sophisticated hyperelastic model than is to be identified can be a good form of model uncertainty. More generally speaking, however, the results indicate the need for a framework that is able to decide by itself to what extent model uncertainty must be applied.

Funding Statement. The project is funded by European Union's Horizon 2020 research and innovation program under the Marie Skłodowska-Curie grant agreement No.764644.

Competing Interests. The authors declare no competing interests exist.

Data Availability Statement. Data have generated artificially as stated in the paper. Rest of the visualization codes and data are available on reasonable request from the corresponding author.

Author Contributions. Conceptualization, S.P.A.B. and L.A.A.B.; Methodology, M.Z.; Formal analysis, L.A.A.B.; Writing-original draft, M.Z.; Writing-review & editing, M.Z. and L.A.A.B.; Supervision, S.P.A.B. and L.A.A.B.; Funding acquisition, S.P.A.B. All authors approved the final submitted draft.

References

Alvin KF (1997) Finite element model update via Bayesian estimation and minimization of dynamic residuals. *AIAA Journal* 35, 879–886.

Arendt PD, Apley DW and Chen W (2012) Quantification of model uncertainty: calibration, model discrepancy, and identifiability. *Journal of Mechanical Design* 134, 100908.

Arhonditsis GB, Papantou D, Zhang W, Perhar G, Massos E and Shi M (2008) Bayesian calibration of mechanistic aquatic biogeochemical models and benefits for environmental management. *Journal of Marine Systems* 73, 8–30.

Beck JL and Katafygiotis LS (1998) Updating models and their uncertainties. I: Bayesian statistical framework. *Journal of Engineering Mechanics* 124, 455–461.

Beex LAA (2019) Fusing the Seth–Hill strain tensors to fit compressible elastic material responses in the nonlinear regime. *International Journal of Mechanical Sciences* 163, 105072.

Beskos A, Pillai N, Roberts G, Sanz-Serna J-M and Stuart A (2013) Optimal tuning of the hybrid Monte Carlo algorithm. *Bernoulli* 19, 1501–1534.

Betancourt M (2017) A conceptual introduction to Hamiltonian Monte Carlo. *Preprint*, arXiv:1701.02434.

Bigoni D, Chen Y, Trillo NG, Marzouk Y and Sanz-Alonso D (2020) Data-driven forward discretizations for Bayesian inversion. *Inverse Problems* 36, 105008.

Bui HP, Tomar S and Bordas SPA (2019) Corotational cut finite element method for real-time surgical simulation: application to needle insertion simulation. *Computer Methods in Applied Mechanics and Engineering* 345, 183–211.

Courtney T, Sacks MS, Stankus J, Guan J and Wagner WR (2006) Design and analysis of tissue engineering scaffolds that mimic soft tissue mechanical anisotropy. *Biomaterials* 27, 3631–3638.

Daghia F, de Miranda S, Ubertini F and Viola E (2007) Estimation of elastic constants of thick laminated plates within a Bayesian framework. *Composite Structures* 80, 461–473.

Duprez M, Bordas SPA, Bucki M, Bui HP, Chouly F, Lleras V, Lobos C, Lozinski A, Rohan P-Y and Tomar S (2020) Quantifying discretization errors for soft tissue simulation in computer assisted surgery: a preliminary study. *Applied Mathematical Modelling* 77, 709–723.

Gogu C, Yin W, Haftka R, Ifju P, Molimard J, Riche RL and Vautrin A (2013) Bayesian identification of elastic constants in multi-directional laminate from Moiré interferometry displacement fields. *Experimental Mechanics* 53, 635–648.

Guo Z, Peng X and Moran B (2006) A composites-based hyperelastic constitutive model for soft tissue with application to the human annulus fibrosus. *Journal of the Mechanics and Physics of Solids* 54, 1952–1971.

Hauseux P, Hale JS, Cotin S and Bordas SPA (2018) Quantifying the uncertainty in a hyperelastic soft tissue model with stochastic parameters. *Applied Mathematical Modelling* 62, 86–102.

Higdon D, Gattiker J, Williams B and Rightley M (2008) Computer model calibration using high-dimensional output. *Journal of the American Statistical Association* 103, 570–583.

Higdon D, Lee H and Bi Z (2002) A Bayesian approach to characterizing uncertainty in inverse problems using coarse and fine-scale information. *IEEE Transactions on Signal Processing* 50, 389–399.

Humphrey JD (2003) Continuum biomechanics of soft biological tissues. *Proceedings of the Royal Society of London. Series A: Mathematical, Physical and Engineering Sciences* 459, 3–46.

Hussein R, Wu L, Noels L and Beex LAA (2019) A Bayesian framework to identify random parameter fields based on the copula theorem and Gaussian fields: application to polycrystalline materials. *Journal of Applied Mechanics* 86, 121009.

Isenberg J (1979) Progressing from least squares to Bayesian estimation. In *Proceedings of the 1979 ASME design engineering technical conference*, New York, 1–11.

Kennedy MC and O'Hagan A (2001) Bayesian calibration of computer models. *Journal of the Royal Statistical Society: Series B (Statistical Methodology)* 63, 425–464.

Koutsourelakis P-S (2012) A novel Bayesian strategy for the identification of spatially varying material properties and model validation: an application to static elastography. *International Journal for Numerical Methods in Engineering* 91, 249–268.

Lai T and Ip K (1996) Parameter estimation of orthotropic plates by Bayesian sensitivity analysis. *Composite Structures* 34, 29–42.

Lan S, Bui-Thanh T, Christie M and Girolami M (2016) Emulation of higher-order tensors in manifold Monte Carlo methods for Bayesian inverse problems, 81–101. *Journal of Computational Physics* 308.

Loew PJ, Peters B and Beex LAA (2020) Fatigue phase-field damage modeling of rubber using viscous dissipation: crack nucleation and propagation. *Mechanics of Materials* 142, 103282.

Loh N and Das M (1986) A unified theory of deterministic system parameter identification. In *ICASSP'86. IEEE International Conference on Acoustics, Speech, and Signal Processing* (Vol. 11, pp. 2707–2710), 2707–2710.

Madireddy S, Sista B and Vemaganti K (2015) A Bayesian approach to selecting hyperelastic constitutive models of soft tissue. *Computer Methods in Applied Mechanics and Engineering* 291, 102–122.

Madireddy S, Sista B and Vemaganti K (2016) Bayesian calibration of hyperelastic constitutive models of soft tissue. *Journal of the Mechanical Behavior of Biomedical Materials* 59, 108–127.

Magliulo M, Lengiewicz J, Zilian A and Beex LAA (2020) Beam-inside-beam contact: mechanical simulations of slender medical instruments inside the human body. *Computer Methods and Programs in Biomedicine* 196, 105527.

Marwala T and Sibisi S (2005) Finite element model updating using Bayesian framework and modal properties. *Journal of Aircraft* 42, 275–278.

McFarland J and Mahadevan S (2008) Multivariate significance testing and model calibration under uncertainty. *Computer Methods in Applied Mechanics and Engineering* 197, 2467–2479.

Mendizabal A, Márquez-Neila P and Cotin S (2020) Simulation of hyperelastic materials in real-time using deep learning. *Medical Image Analysis* 59, 101569.

Mohamedou M, Zulueta K, Chung CN, Rappel H, Beex LAA, Adam L, Arriaga A, Major Z, Wu L and Noels L (2019) Bayesian identification of mean-field homogenization model parameters and uncertain matrix behavior in non-aligned short fiber composites. *Composite Structures* 220, 64–80.

Nichols J, Link W, Murphy K and Olson C (2010) A Bayesian approach to identifying structural nonlinearity using free-decay response: application to damage detection in composites. *Journal of Sound and Vibration* 329, 3927–3941.

Ortiz A, Banks H, Castillo-Chávez C, Chowell G and Wang X (2011) A deterministic methodology for estimation of parameters in dynamic Markov chain models. *Journal of Biological Systems* 19, 71. <http://dx.doi.org/10.1142/s0218339011003798>

Rappel H and Beex LAA (2019) Estimating fibres' material parameter distributions from limited data with the help of Bayesian inference. *European Journal of Mechanics—A/Solids* 75, 169–196. Available at <http://www.sciencedirect.com/science/article/pii/S0997753818305916>. <https://doi.org/10.1016/j.euromechsol.2019.01.001>

Rappel H, Beex LAA and Bordas SPA (2018) Bayesian inference to identify parameters in viscoelasticity. *Mechanics of Time-Dependent Materials* 22, 221–258.

Rappel H, Beex LAA, Hale JS, Noels L and Bordas SPA (2020) A tutorial on Bayesian inference to identify material parameters in solid mechanics. *Archives of Computational Methods in Engineering*. 2020 Apr;27(2):361–385.

Rappel H, Beex LAA, Noels L and Bordas SPA (2019) Identifying elastoplastic parameters with Bayes' theorem considering output error, input error and model uncertainty. *Probabilistic Engineering Mechanics* 55, 28–41.

Risholm P, Janoos F, Norton I, Golby AJ and Wells WM (2013) Bayesian characterization of uncertainty in intra-subject non-rigid registration. *Medical Image Analysis* 17, 538–555.

Ritto T and Nunes L (2015) Bayesian model selection of hyperelastic models for simple and pure shear at large deformations. *Computers & Structures* 156, 101–109.

Sankararaman S, Ling Y, Shantz C and Mahadevan S (2011) Inference of equivalent initial flaw size under multiple sources of uncertainty. *International Journal of Fatigue* 33, 665–680.

Teferra K and Brewick PT (2019) A Bayesian model calibration framework to evaluate brain tissue characterization experiments. *Computer Methods in Applied Mechanics and Engineering* 357, 112604.

Wang J and Zabaras N (2004) A Bayesian inference approach to the inverse heat conduction problem. *International Journal of Heat and Mass Transfer* 47, 3927–3941.

Wu J-Y and Lee T-S (2006) Optimal least squares deterministic parameter estimation from a class of block-circulant-with-circulant-block linear model. In *2006 IEEE International Symposium on Information Theory*. IEEE, 846–850.